Memory-induced resonancelike suppression of spike generation in a resonate-and-fire neuron model

Romi Mankin and Sander Paekivi*
School of Natural Sciences and Health, Tallinn University, 29 Narva Road, 10120 Tallinn, Estonia

(Received 31 July 2017; revised manuscript received 3 November 2017; published 18 January 2018)

The behavior of a stochastic resonate-and-fire neuron model based on a reduction of a fractional noise-driven generalized Langevin equation (GLE) with a power-law memory kernel is considered. The effect of temporally correlated random activity of synaptic inputs, which arise from other neurons forming local and distant networks, is modeled as an additive fractional Gaussian noise in the GLE. Using a first-passage-time formulation, in certain system parameter domains exact expressions for the output interspike interval (ISI) density and for the survival probability (the probability that a spike is not generated) are derived and their dependence on input parameters, especially on the memory exponent, is analyzed. In the case of external white noise, it is shown that at intermediate values of the memory exponent the survival probability is significantly enhanced in comparison with the cases of strong and weak memory, which causes a resonancelike suppression of the probability of spike generation as a function of the memory exponent. Moreover, an examination of the dependence of multimodality in the ISI distribution on input parameters shows that there exists a critical memory exponent $\alpha_c \approx 0.402$, which marks a dynamical transition in the behavior of the system. That phenomenon is illustrated by a phase diagram describing the emergence of three qualitatively different structures of the ISI distribution. Similarities and differences between the behavior of the model at internal and external noises are also discussed.

DOI: 10.1103/PhysRevE.97.012125

I. INTRODUCTION

Noise-induced phenomena in complex systems present a fascinating subject of investigation since, contrary to intuition, environmental randomness may induce more order in the behavior of the system. Stochastic resonance [1,2], the ratchet effect [3,4], anomalous diffusion [5–7], and noise-enhanced stability [8,9] are a few examples in this field. An object of special attention in this context is the noise-driven fractional oscillator. As oscillators are simple toy models for different phenomena in nature, they tend to serve as a theoretician's typical paradigm for various fundamental conceptions [10].

The fractional oscillator is a generalization of the harmonic oscillator where the usual friction term in the dynamical equation is replaced by a generalized friction term with a power-law memory kernel [5,11–14]. The dynamical equation for such an oscillator is a special case of the generalized Langevin equation (GLE) (see, e.g., [15]). The main advantage of this equation is that it provides a physically transparent and mathematically tractable description of the stochastic dynamics in systems with slow relaxation processes and anomalously slow diffusion (subdiffusion). Examples of such systems are colloidal suspensions, glasses, polymer solutions [16,17], viscoelastic media, amorphous semiconductors [18–20], cytoplasm of living cells [21], large proteins [22], and dusty plasmas [23]. Also, diffusion on fractal structures and on percolating clusters is anomalously slow [24,25] and thus belongs on this list.

Noise-dependent behavior of neural systems has received considerable attention [26–38]. Since the classical four-dimensional Hodgkin-Huxley neuron model requires nearly 20 parameters to be determined [39], stochastic versions for reduced models of neurons, which capture the essence of the electrical activity of a generic neuron, are more interesting from both analytical and computational points of view. Moreover, an understanding of neuronal mechanisms gained from reduced models could be useful in the engineering of artificial neural devices designed to reproduce a given real biological feature [40]. Two important classes of such models are the integrate-and-fire (IF) [27,28] and the resonate-and-fire (RF) [29,41–44] models. The RF model is more flexible than the IF one (included in the RF model as a special case) and as such is able to describe the dynamics of a larger class of neural systems. It should be emphasized that the dynamics of stochastic RF models is closely linked to the dynamical behavior of noise-driven harmonic and anharmonic oscillators [41,44].

Until relatively recently, most of the stochastic models studied analytically in neuroscience had focused on Gaussian white noise as well as on shot noise with exponentially distributed weight input [27,28]. However, the real effective random influence of other neurons on the synaptic inputs of cortical neurons should be considered as a colored-noise-generated process, where the stimulation from other neurons is temporally correlated [30,37,45]. For example, pronounced input correlations in time arise because of temporally correlated input stimuli, presynaptic refractoriness or bursting, adaptation, network-generated oscillations, and short-term synaptic plasticity [37]. From the theoretical side, it is poorly understood how these correlated stimuli affect the statistical structure of neural spiking. Most of the analytical results for the cases of input colored noises have been obtained for limits of slow and fast noises [35], as well as in a weak-noise approximation

*sander.paekivi@tlu.ee

 ©2018 American Physical Society

[32,36]. The dichotomous Markov process [46], a two-state noise with an exponential correlation function, is the rare example of a driving colored noise that can lead to exact results for IF neurons [33,35,37,47,48].

As mentioned above, the simplest possible formulation of the RF model is based on the dynamics of the harmonic oscillator driven by Gaussian white noise. The corresponding Langevin equation is characterized by Gaussian white noise and by time-local dissipative terms. This assumption is valid only for particular limit cases. A more realistic description of neural networks requires taking into account that information exchange takes place during finite-time intervals, which must lead to finite-memory effects and colored noise. One of the possibilities of modeling such processes can be formulated in the framework of a GLE, where a nonlocal dissipative term (memory kernel) and correlated noise reflect finite-time effects.

Recently, a generalization of the stochastic RF model to the context of a GLE model with an exponential memory kernel, driven by Ornstein-Uhlenbeck noise, was proposed in [40]. The comprehensive numerical simulation put forth in this paper reveals a set of important features of the interspike interval (ISI) distribution and of the coefficient of variation that stems from the interplay between memory and colored noise. For example, the emergence and suppression of multimodality in the ISI distribution due to memory-induced subthreshold oscillations was established, thus suggesting that memory can be seen as an effective mechanism for generating and controlling neuron variability [40]. We would note that it is empirically known that the ISI density of real neurons (e.g., pallidal and ganglion cells) can exhibit nontrivial patterns, such as a bimodal or multimodal structure depending on the input [40,49,50]. However, in Ref. [40] it is assumed that the memory kernel in the GLE is characterized by a decaying exponential function. The latter is irrelevant for neural networks with fractal structure, where anomalous diffusion occurs. As recent investigations indicate, some structures of complex brain neural networks have a fractal character [51–53], thus it is of interest, from both theoretical and possible experimental viewpoints, to know the behavior of the ISI statistics of a stochastic RF model subject to a power-law memory kernel.

In the present paper, inspired by the results of [40,51] and by the reasons presented above, we consider an RF model based on the dynamics of a fractional oscillator, where the effect of temporally correlated random neuronal inputs is modeled as a fractional Gaussian noise. The idea of the proposed model is to describe the neuron membrane potential $v(t)$ dynamics by a time-nonhomogeneous one-dimensional (1D) Langevin equation driven by white Gaussian noise, which is equivalent to the basic stochastic fractional oscillator in the sense that their one-time statistical properties in v space are identical. The main contribution of this paper is as follows. We provide, in the noise-induced spiking regime of the neuron, exact analytical formulas for the dependence of some statistical characteristics of the output spike train, such as the probability distribution of the ISIs and the survival probability, on the parameters of the input stimulus. On the basis of the exact expressions, we have found two qualitatively different shapes of the ISI distribution: one unimodal and the other multimodal. Furthermore, we establish sufficient conditions for the validity of the obtained formulas for the ISI density and analyze the corresponding dynamical phase diagram in the system parameter space. In particular, memory-induced transitions between unimodal and multimodal structures of the ISI density and a critical memory exponent which marks a dynamical transition in the behavior of the system are found. Moreover, in the case of external white noise, we demonstrate that at intermediate values of the memory exponent, the survival probability is significantly enhanced compared to the cases of strong and weak memory, which cause a resonancelike suppression of the probability of spike generation as a function of the memory exponent. We also show that in the case of internal noise, the just-mentioned phenomenon is absent, as in this case the survival probability is independent of the memory exponent.

The structure of the paper is as follows. In Sec. II, we present the model investigated. In Sec. III, exact formulas are found for the ISI statistics. In Sec IV, we discuss the behavior of the statistical measures and illustrate their characteristic features. Section V contains a summary. Some formulas are given in the Appendixes.

II. MODEL

Damped fast subthreshold oscillations of the membrane potential have been observed in many biological neurons (see, e.g., [43,54,55] and references therein). This dynamical property makes neurons sensitive to the timing of a stimulus and may lead to many interesting phenomena [41]. This property also occurs in almost all biophysically detailed Hodgkin-Huxley-type neural models, but is obscured by the complexity of the models and may be difficult to understand and simulate, especially in a network of neurons [41]. From a dynamical viewpoint, such subthreshold oscillations occur when the neurons operate close to an Andronov-Hopf bifurcation. Several reduced mathematical models of neurons (called resonate-and-fire neuron models) have been used as tools for the analysis of the aforementioned subthreshold oscillations taking place in the complex activity of neurons and their networks [40–43]. This kind of model is typically characterized by a second-order differential equation whose solution describes the time evolution of the subthreshold membrane potential and an *ad hoc* rule according to which, when the potential reaches the threshold, a spike is produced and the potential is reset to a certain value representing the effect of the inward-rectifier potassium channel [34,40]. More precisely, in the Hodgkin-Huxley model, the reset rule reflects the biophysical fact that, subsequent to a spike, all neuron state variables return to a small region in the phase space. In the RF model, the reset rule corresponds to the simplification that replaces this small region by a single point. Although an RF model is a gross oversimplification of any actual neural system, it adequately describes the general features of the ISI statistics for some neurons [41–43].

Before addressing the RF model proposed in the present paper, let us briefly review the main features of the underlying GLE model and the role of the reset rule in the stochastic process associated with this GLE. We consider a fractional oscillator subjected to an external input force, proportional to the current, consisting of two parts, the constant average $\mu > 0$

and a fluctuating part $\xi(t)$, as

$$\ddot{v}(t) + \gamma \frac{d^\alpha}{dt^\alpha} v(t) + \omega^2 v(t) = \mu + \xi(t), \tag{1}$$

where $\dot{v} \equiv \frac{dv}{dt}$, $v(t)$ is the membrane potential at time t, γ is a damping constant, the square of the eigenfrequency ω can be interpreted in mechanical terms as the stiffness of an effective trapping potential

$$U_{\text{eff}} = \frac{\omega^2}{2} v^2 - \mu v, \tag{2}$$

and the operator $\frac{d^\alpha}{dt^\alpha}$ with a memory exponent α denotes the fractional derivative in Caputo's sense, given by [56]

$$\frac{d^\alpha}{dt^\alpha} v(t) = \frac{1}{\Gamma(1-\alpha)} \int_0^t \frac{\dot{v}(t')}{(t-t')^\alpha} dt', \tag{3}$$

$\Gamma(y)$ being the Gamma function and $0 < \alpha < 1$. Fluctuations of the input force, which arise from other neurons forming a fractal network, are expressed as a stationary fractional Gaussian noise $\xi(t)$ with a zero mean $\langle \xi(t) \rangle = 0$ and a correlation function

$$\langle \xi(t)\xi(t') \rangle = C(|t-t'|) = \frac{D}{\Gamma(1-\beta)|t-t'|^\beta}, \tag{4}$$

where D characterizes the noise intensity and $0 < \beta < 1$. Depending on the physical situation, the driving noise $\xi(t)$ can be regarded either as an internal noise (thermal noise) or as an external noise. If the noise $\xi(t)$ is internal, the dissipative memory kernel

$$\eta(\tau) = \frac{1}{\Gamma(1-\alpha)\tau^\alpha} \tag{5}$$

arising in Eq. (1) due to the fractional derivative $d^\alpha v(t)/dt^\alpha$ [see also Eq. (3)] is related to the noise correlation function $C(|\tau|)$ via Kubo's second fluctuation-dissipation theorem [57]

$$C(|\tau|) = k_B T \gamma \eta(|\tau|), \tag{6}$$

where T is the absolute temperature of the heat bath and k_B is the Boltzmann constant. This means that the fluctuations and dissipation come from the same source, i.e., due to the impact of the environment on the particle. In this case the system described by the GLE (1) with Eq. (6) reaches a state of thermal equilibrium. Note that when the noise $\xi(t)$ is internal, from Eqs. (4)–(6) it follows that the noise exponent is the same as the memory exponent, $\beta = \alpha$. In the case of external noise however, the driving noise $\xi(t)$ and dissipation may have different origins and no fluctuation-dissipation relation holds, in this case $\beta \neq \alpha$. By taking the limit $\beta \to 1$ in Eq. (4), we can see that the correlation function (4) possesses all the properties of the δ function (its δ-functional behavior manifests itself in the integrals) and thus the noise $\xi(t)$ corresponds to white noise and consequently, in the case of internal noise, to nonretarded friction in the GLE (1).

Equation (1), describing the subthreshold evolution of the membrane potential, is the basic equation of this paper. We adopt the following fire-and-reset rule: If the voltage reaches a certain threshold value $v(t) = v_c$, then a spike is considered to have occurred at time t and the voltage is reset to the state

$$v = v_r = \frac{\mu}{\omega^2}, \quad \dot{v} = \dot{v}_r = 0, \tag{7}$$

which corresponds, in the case without noise, to the equilibrium state, i.e., to the minimum of the effective potential U_{eff} [cf. Eq. (2)]. As the reset state is a stable equilibrium for the solutions of the deterministic version of Eq. (1), to make the neuron fire ($v = v_c$), external perturbations [the noise $\xi(t)$ in Eq. (1)] should push $v(t)$ far enough from the reset state. Thus, in the proposed model, the probability of spike occurrence is non-null only in the stochastic case. One refers to this case as the noise-induced firing regime of a neuron. The main source of information about the dynamics of a neuron is the ISI distribution. This distribution equals the probability density of the time needed to reach the voltage threshold for the first time after starting at the reset value. Obtaining such a distribution is known as a first-passage-time (FPT) approach (see, e.g., [42]).

Unfortunately, the process $v(t)$ described by Eq. (1) is highly non-Markovian and there does not exist a finite-dimensional supplementary variable representation to make it Markovian. As a result of the intrinsically non-Markovian character of Eq. (1), the determination of its FPT distribution becomes difficult and so far no exact results have been obtained (see also [58]).

Various methods have been used to approximately determine the FPT distribution of non-Markovian processes [42,58]. As an example, perhaps more important in the context of RF models, we mention here Ref. [42], where a general expression for the FPT density for stochastic processes with differentiable trajectories is given. As this expression results in an infinite series of integrals over joint densities of multiple level crossings, some approximations based on the truncation or an approximate summation of this series are necessary for calculations. To improve the reliability of an approximation, a large number of terms needs to be calculated semianalytically and then the computational cost for obtaining the approximate results rapidly approaches the one for simulating the dynamical equations [40,42].

In the present paper we propose, based on the dynamical equation (1), an alternative RF model, which is able to mimic some crucial aspects of RF models, such as a bimodal or multimodal structure of the ISI distribution depending on the input. The proposed 1D model is Markovian and is fully characterizable by a Fokker-Planck equation (FPE), which coincides exactly with the master equation for the one-time conditional probability densities of the process $v(t)$ described by Eq. (1) [see Appendix A, Eq. (A7)]. The main advantage of this model is that, in some parameter regimes, it enables one to derive exact analytical expressions for the FPT density. However, it should be pointed out that writing an FPE for a non-Markovian system is a simplification (effects of multitime statistical characteristics of the non-Markovian process are ignored) that in general can give different results for FPT densities.

Inspired by the original idea of Gerstein and Mandelbrot [26] to describe neuronal activity by a stochastic perfect integrate-and-fire model driven by a Gaussian white noise, where the key quantity is the one-time probability density in v space, we consider an ordinary overdamped Langevin equation with explicitly time-dependent drift and diffusion terms

$$dv(t) = A(t)dt + \sqrt{2D(t)}dW(t), \tag{8}$$

where $W(t)$ is a Wiener process, as an RF model for membrane potential dynamics. The functions $A(t)$ and $D(t)$ are determined from Eq. (1) by the condition that one-time conditional probability densities in v space, $p(v,t|v_0,\dot{v}_0,0)$, for both processes described by Eqs. (1) and (8), respectively, coincide in all values of time $t \geqslant 0$ (see also Appendix A). More precisely, in Appendix A we show that in the case of $\dot{\sigma}_{vv}(t) \geqslant 0$ the appropriate drift and diffusion terms $A(t)$ and $D(t)$ are given by the equations

$$A(t) = \langle \dot{v}(t) \rangle, \quad D(t) = \tfrac{1}{2}\dot{\sigma}_{vv}(t), \tag{9}$$

where the variance $\sigma_{vv}(t) = \langle [v(t) - \langle v(t) \rangle]^2 \rangle$ and the mean $\langle v(t) \rangle$ can be obtained with the help of Eq. (1) and the angular brackets denote averaging over an ensemble of realizations of the noise $\xi(t)$ (see also Sec. III). Since the process described by Eq. (8) is Markovian, $v(t)$ is fully characterized by an FPE. Thus the FPT distribution of $v(t)$ can be determined by considering the effective FPE with an appropriate boundary condition [59], which is equivalent to the fire-and-reset rule. Since we are interested in the first arrival time at which this process reaches a threshold v_c for the first time, we consider the process up to that time and then kill it by absorption. In other words, one works with an absorbing boundary at $v = v_c$, i.e.,

$$p(v_c,t|v_0,\dot{v}_0,0) = 0. \tag{10}$$

Finally, we again point out that although the dynamics (and also the corresponding FPT distributions) of the stochastic differential equations (SDEs) (1) and (8) are different, they are equivalent in the sense that their one-time statistical properties in v space should be identical. Therefore, Eq. (8) with Eq. (9) also describes the position v of a 1D Brownian particle evolving with time in the GLE (1) picture.

III. EXACT ISI DISTRIBUTION

To find FPT statistics, such as the survival probability and the FPT density, we start from a description of the evolution of the statistical moments for the voltage $v(t)$ determined by Eq. (1).

A. First and second moments

To find the statistical moments of $v(t)$ we follow the calculation scheme described in Ref. [13]. The second-order differential equation (1) can be written as two first-order equations for $v(t)$ and $y(t) = \dot{v}(t)$, which, after averaging over the ensemble of realizations of the random process $\xi(t)$, take the following form:

$$\langle v(t) \rangle^{\cdot} = \langle y(t) \rangle,$$
$$\langle y(t) \rangle^{\cdot} + \gamma \int_0^t \eta(t-t')\langle y(t') \rangle dt' + \omega^2 \langle v(t) \rangle = \mu. \tag{11}$$

Here we have used that the noise $\xi(t)$ is zero centered. Thus, it turns out that fluctuations of the driving random force $\xi(t)$ do not affect the first moments $\langle v(t) \rangle$ and $\langle \dot{v}(t) \rangle$ of the voltage and $\langle v(t) \rangle$ remains equal to the noise-free solution. By applying the Laplace transformation to Eq. (1), one can easily obtain formal expressions for the oscillator displacement $v(t)$ and the velocity $\dot{v}(t)$ in the following forms:

$$v(t) = \langle v(t) \rangle + \int_0^t H(t-\tau)\xi(\tau)d\tau, \tag{12}$$

$$\dot{v}(t) = \langle \dot{v}(t) \rangle + \int_0^t \dot{H}(t-\tau)\xi(\tau)d\tau, \tag{13}$$

where the averages $\langle v(t) \rangle$ and $\langle \dot{v}(t) \rangle$ are given by

$$\langle v(t) \rangle = \frac{\mu}{\omega^2} + \dot{v}_0 H(t) + \left(v_0 - \frac{\mu}{\omega^2}\right) \times \left(1 - \omega^2 \int_0^t H(\tau)d\tau\right) \tag{14}$$

and

$$\langle \dot{v}(t) \rangle = \dot{v}_0 \dot{H}(t) - \omega^2 \left(v_0 - \frac{\mu}{\omega^2}\right) H(t), \tag{15}$$

respectively, with deterministic initial conditions $v(0) = v_0$ and $\dot{v}(0) = \dot{v}_0$ (see also Appendix B). The kernel $H(t)$ with the initial conditions $H(0) = 0$ and $\dot{H}(0) = 1$ is the Laplace inversion of

$$\hat{H}(s) = \frac{1}{s^2 + \gamma s^\alpha + \omega^2}, \tag{16}$$

where

$$\hat{H}(s) = \int_0^\infty e^{-st} H(t)dt. \tag{17}$$

From Eqs. (12) and (13), also taking into account the symmetry of the correlation function $C(|t-t'|)$, it is easy to obtain explicit expressions for the second moments $\sigma_{vv}(t) = \langle [v(t) - \langle v(t) \rangle]^2 \rangle$, $\sigma_{yy}(t) = \langle [\dot{v}(t) - \langle \dot{v}(t) \rangle]^2 \rangle$, and $\sigma_{yv} = \langle [\dot{v}(t) - \langle \dot{v}(t) \rangle][v(t) - \langle v(t) \rangle] \rangle$ of the process (1):

$$\sigma_{vv}(t) = 2\int_0^t H(t_1)M(t_1)dt_1, \tag{18}$$

$$\sigma_{yy}(t) = 2\int_0^t \dot{H}(t_1)\dot{M}(t_1)dt_1, \tag{19}$$

$$\sigma_{yv}(t) = \frac{1}{2}\dot{\sigma}_{vv}(t) = M(t)H(t), \tag{20}$$

where

$$M(t) = \int_0^t H(t-t_1)C(t_1)dt_1. \tag{21}$$

In the case of internal noise, Eqs. (18)–(20) can be simplified to (cf. also Ref. [13])

$$\sigma_{vv}(t) = \frac{k_B T}{\omega^2}[1 - \omega^2 H^2(t) - \omega^4 (G(t))^2], \tag{22}$$

$$\sigma_{yy}(t) = k_B T[1 - \dot{H}^2(t) - \omega^2 H^2(t)], \tag{23}$$

$$\sigma_{yv}(t) = k_B T H(t)[\omega^2 G(t) - \dot{H}(t)], \tag{24}$$

where

$$G(t) = \int_t^\infty H(t')dt'. \tag{25}$$

An integral representation of the relaxation functions $H(t)$, $M(t)$, and $G(t)$ is given by Eqs. (B6)–(B15) in Appendix B.

Due to the Gaussian property of the noise $\xi(t)$ and the linearity of Eq. (1), the joint probability density $p(v,\dot{v},t)$ must also be Gaussian. The marginal probability density $P(v,t) \equiv p(v,t|v_0,\dot{v}_0,0)$ for the process $v(t)$ with deterministic initial conditions $v(0) = v_0$ and $\dot{v}(0) = \dot{v}_0$ satisfies the master equation [13]

$$\frac{\partial}{\partial t}P(v,t) = -\langle \dot{v}(t)\rangle \frac{\partial}{\partial v}P(v,t) + \sigma_{yv}(t)\frac{\partial^2}{\partial v^2}P(v,t), \quad (26)$$

where $\langle \dot{v}(t)\rangle$ and σ_{yv} are determined by Eqs. (15) and (20), respectively (see Appendix A). Equation (26), with Eqs. (15) and (20), is crucial for solving the FPT problem to obtain the ISI distribution generated by the model (8) and (9). Here we emphasize that Eq. (26) is the exact Fokker-Planck equation for the SDE (8) with Eq. (9).

B. First-passage-time distributions

From now on, we consider the FPT problem for the reduced RF model (8) and (9), which is the main goal of the present paper. First, we recall that since the process described by Eq. (8) is Markovian, the evolution of the voltage $v(t)$ is fully characterized by the FPE (26) with the notation $P(v,t) \equiv p(v,t|v_0,\dot{v}_0,0)$ [cf. Eq. (A7)]. As mentioned above, for the subthreshold voltage evolution process $v(t)$ commencing at the reset state [see Eq. (7)] at $t = 0$, the time at which this process reaches the threshold v_c for the first time is itself a random variable whose statistics are fundamental for the ISI distribution. The FPT problem from $v = v_r = \frac{\mu}{\omega^2}$ and $\dot{v} = \dot{v}_r = 0$ to $v = v_c > \frac{\mu}{\omega^2}$ is associated with a solution of the FPE (26) with the δ-distributed initial condition

$$P(v,0) = \delta\left(v - \frac{\mu}{\omega^2}\right) \quad (27)$$

in the presence of an absorbing boundary at $v = v_c$,

$$P(v_c,t) = 0. \quad (28)$$

Using the conditions (7), from Eq. (15) one can see that the average $\langle \dot{v}(t)\rangle$ vanishes, i.e., $\langle \dot{v}(t)\rangle = 0$ for $t \geqslant 0$, and Eq. (26) reduces to a diffusion equation without drift and with the time-dependent diffusion coefficient $\sigma_{yv}(t)$. The corresponding normalized solution of Eq. (26) with the initial condition (27) for an unrestricted process (without an absorbing boundary), starting from the reset state, can be obtained as

$$P_u(v,t) = \frac{1}{\sqrt{2\pi\sigma_{vv}(t)}}\exp\left[-\frac{(v-\mu/\omega^2)^2}{2\sigma_{vv}(t)}\right]. \quad (29)$$

If the condition

$$\sigma_{yv}(t) = H(t)M(t) \geqslant 0 \quad (30)$$

is fulfilled in the time interval $(0,t)$, then in the same interval, Eq. (26), with the absorbing boundary at v_c and with the initial condition (27), can be readily solved by the method of images with a mirror source at $v = 2v_c - \mu/\omega^2$ [59]. The solution can be written as

$$P(v,t) = \frac{1}{\sqrt{2\pi\sigma_{vv}(t)}}\left[\exp\left(-\frac{(v-\mu/\omega^2)^2}{2\sigma_{vv}(t)}\right) - \exp\left(-\frac{(v-2v_c+\mu/\omega^2)^2}{2\sigma_{vv}(t)}\right)\right], \quad (31)$$

where $-\infty < v \leqslant v_c$. The survival probability $F(t)$ is defined as the probability of the process trajectories not being absorbed before time t [or the probability that a spike is not generated in the interval $(0,t)$],

$$F(t) = \int_{-\infty}^{v_c} P(v,t)dv = \mathrm{erf}\left(\frac{v_c - \mu/\omega^2}{\sqrt{2\sigma_{vv}(t)}}\right), \quad (32)$$

where $\mathrm{erf}(y)$ is the standard normal integral

$$\mathrm{erf}(y) = \frac{2}{\sqrt{\pi}}\int_0^y e^{-x^2}dx. \quad (33)$$

The FPT density (or the ISI distribution) $w(t|v_c)$ is given by

$$w(t|v_c) = -\dot{F}(t) = \frac{\sqrt{2}H(t)M(t)(v_c-\mu/\omega^2)}{\sqrt{\pi}[\sigma_{vv}(t)]^{3/2}} \times \exp\left[-\frac{(v_c-\mu/\omega^2)^2}{2\sigma_{vv}(t)}\right], \quad (34)$$

if $\dot{\sigma}_{vv}(t) = 2H(t)M(t) \geqslant 0$ [cf. Eq. (30)]. Particularly in the case of Gaussian white noise $\xi(t)$ [$\beta \to 1$ in Eq. (4)] the inequality (30) is always fulfilled and the formulas (32) and (34) are consequently applicable for all values of time $t \in (0,\infty)$. Since in the limit $t \to \infty$ the variance $\sigma_{vv}(t)$ saturates to a finite value (except for some very special parameter regimes) $0 < \sigma_{vv}(\infty) < \infty$, then, as a rule, the survival probability $F(\infty)$ is not zero, i.e., there is a finite probability that a spike is not generated in the time interval $(0,\infty)$. Thus $w(t|v_c)dt$ is actually the joint probability for two events: that a spike is generated at all and that this spike appears in the interval $(t,t+dt)$. Evidently, one obtains

$$\int_0^\infty w(t|v_c)dt = 1 - F(\infty). \quad (35)$$

Although the integral (35) is not normalized to 1, for convenience we will henceforth refer to $w(t|v_c)$ as the ISI density (or FPT density).

The exact formulas (32), (34), and (35) are the main analytical results of the present paper, as they permit the analysis of the role of memory in the behavior of the ISI distribution, as well as the calculation of the statistical moments of interspike intervals. In particular, those formulas are crucial to establish the phenomenon of memory-induced resonancelike suppression of the probability of spike generation (see Sec. IV B).

IV. RESULTS

A. Memory-induced transitions

As mentioned in Sec. III, the inequality (30) is crucial for the derivation of the ISI distribution (34). Assuming that the correlation function $\langle \xi(t)\xi(t')\rangle$ of the colored noise $\xi(t)$ [e.g., $\beta \neq 1$ in Eq. (4)] is non-negative, which is the case considered in this paper [see Eq. (4)], from Eqs. (20), (21), and (30) one can see that the inequality (30) is fulfilled in the time interval $(0,t)$ if and only if

$$H(t') \geqslant 0 \quad (36)$$

for all $t' \in (0,t)$. Thus, we can discern two cases: (i) the case where the condition (36) is valid in the whole semiaxis, i.e., $t' \in (0,\infty)$, and (ii) the case where Eq. (36) is only valid in a finite interval $(0,t)$.

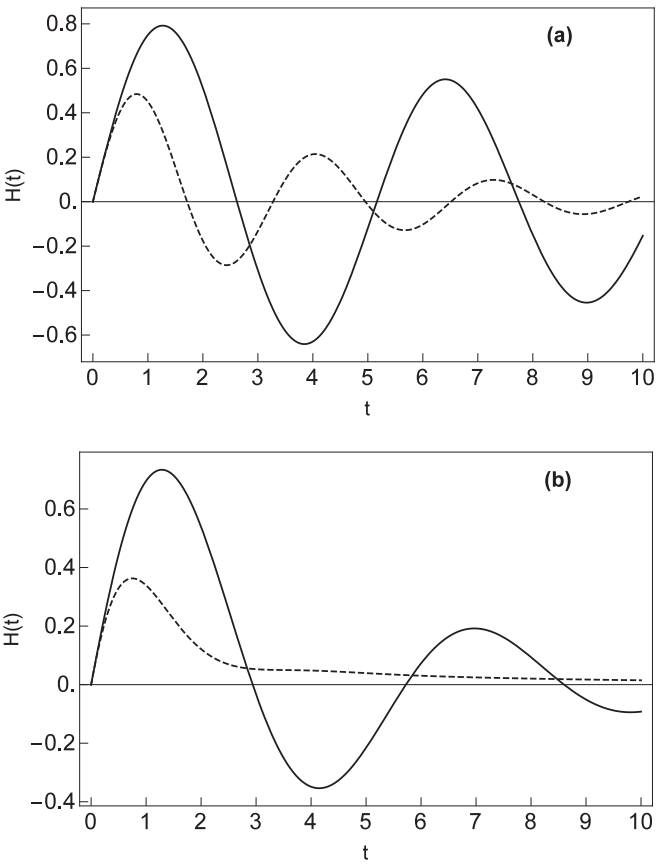

FIG. 1. Behavior of the relaxation function $H(t)$ computed from Eqs. (B6)–(B12) for various values of the memory exponent α and the damping constant γ: (a) $\alpha = 0.2$ and $\gamma = 0.5$ (solid line) and $\alpha = 0.2$ and $\gamma = 2.5$ (dashed line) and (b) $\alpha = 0.7$ and $\gamma = 0.5$ (solid line) and $\alpha = 0.7$ and $\gamma = 2.5$ (dashed line). Note the absence of sign reversals of $H(t)$ in (b) at $\gamma = 2.5$ (dashed line). All quantities are dimensionless, with time scaling determined by $\omega = 1$.

In Figs. 1(a) and 1(b) we depict the dependence of the relaxation function $H(t)$ for various values of the damping constant γ and the memory exponent α on time t. From Fig. 1 one notices that there are two different types of oscillating behaviors of $H(t)$, one with zero crossings and the other without. It is seen that, contrary to the case of low values of the memory exponent ($\alpha = 0.2$ in Fig. 1), where the sign reversals of $H(t)$ versus t occur for any γ, at relatively high values of α ($\alpha = 0.7$ in Fig. 1) and the damping coefficient γ the relaxation function $H(t)$ is positive for all values of t.

This indicates that in the phase space of the system parameters (γ,ω,α), a critical surface $\gamma_c(\alpha,\omega)$ should exist, which divides the phase space into two different regions: a region where the relaxation function $H(t)$ is non-negative and one where it exhibits sign reversals. In order to find such a critical surface, two conditions must be satisfied:

$$H(t) = 0, \quad \dot{H}(t) = 0. \tag{37}$$

Using Eqs. (B16) and (B17), we find in Appendix B from dimensional analysis

$$\frac{\gamma_c}{\omega^{2-\alpha}} = \kappa(\alpha), \tag{38}$$

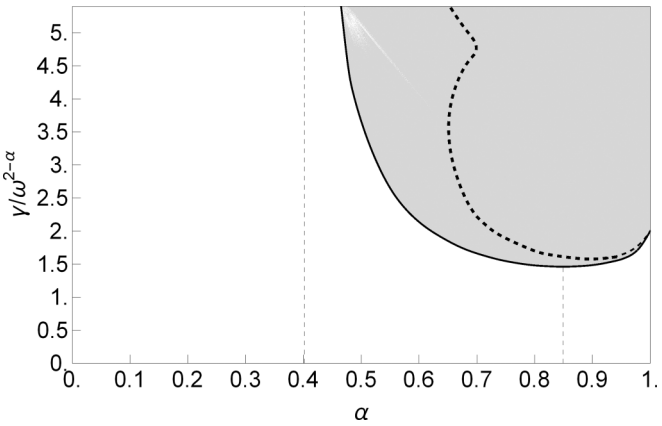

FIG. 2. Phase diagram of the fractional oscillator (1). In the shaded region, the relaxation function $H(t)$ [see Eqs. (16) and (17)] is always non-negative. In the unshaded domain, sign reversals of $H(t)$ occur. The critical curve (solid line) $\gamma_c/\omega^{2-\alpha} = \kappa(\alpha)$ [see Eq. (38)] tends to infinity at $\alpha = \alpha_c \approx 0.402$. The thin dotted lines mark the positions of the critical exponent α_c and the minimal value of $\kappa(\alpha)$, respectively; $\min \kappa(\alpha) = \kappa(\alpha_m) \approx 1.461$ with $\alpha_m \approx 0.849$. The bold dashed line marks another critical curve $\gamma_{c1}/\omega^{2-\alpha} = \kappa_1(\alpha)$ above which the ISI distribution (34) is, in the case of internal noise at system parameters $k_B T = 0.15$, $\omega = \mu = 1$, and $v_c = 1.75$, unimodal.

where the function $\kappa(\alpha)$ depends only on the memory exponent α. By investigating the analytical solutions of $H(t)$ [Eqs. (B6)–(B12)] numerically for various values of α and with $\omega = 1$, we obtain from the conditions (37) a numerical representation of the function $\kappa(\alpha)$. The resulting phase diagram is represented in Fig. 2. The shaded region on the phase diagram corresponds to the system parameter domain where $H(t) \geqslant 0$ for all values of t; in the unshaded region, the sign reversals of $H(t)$ versus t occur. In the limit of vanishing memory $\alpha \to 1$, the critical curve $\kappa(\alpha)$ tends to the value 2, which reflects the well-known dynamics transition of the ordinary harmonic oscillator from an underdamped regime to an overdamped regime (the corresponding critical damping constant for the ordinary oscillator is $\gamma_c = 2\omega$). An important behavior is observed for $\kappa(\alpha)$: As can be seen in Fig. 2, a phase transition occurs around $\alpha = \alpha_c \approx 0.402$. If $\alpha \to \alpha_c$, the value of $\kappa(\alpha)$ tends to infinity and consequently for $\alpha < \alpha_c$, the relaxation function exhibits sign reversals versus time t for all values of the other system parameters.

It should be noted that previously, the same value of the critical memory exponent, $\alpha_c \approx 0.402$, was obtained by analysis of the normalized correlation function of a fractional oscillator in Ref. [11], but the connection between the phase diagram and the behavior of the relaxation function was not considered there. In this reference, based on the cage effect [7,11], we also find a physical explanation for the role of the memory exponent α in the dynamics of the fractional oscillator. Namely, from a mechanical point of view, for small α the friction force induced by a viscoelastic medium [the nonlocal fractional derivative in Eq. (1)] is not just slowing down the particle but also causing the particle to undergo a rattling motion, which can be explained by the harmonic motion of the particle in a cage formed by the surrounding particles [11]. Here, at small α the medium is binding the particle, thus

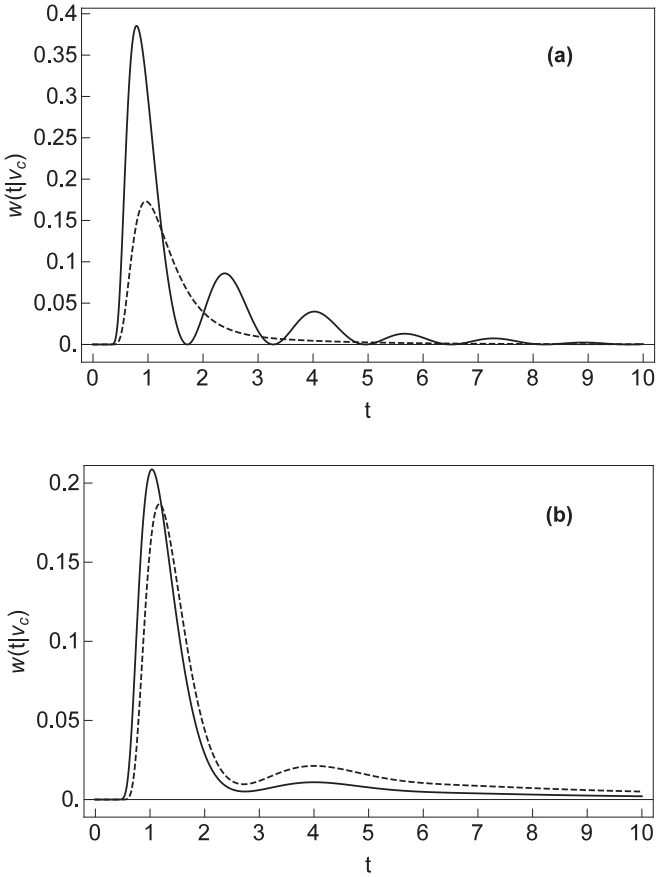

FIG. 3. The ISI distribution $w(t|v_c)$ versus time t [see Eq. (34)]. All quantities are dimensionless, with time and voltage scaling determined by $\omega = 1$ and $\mu = 1$, respectively. The system parameter values are $\gamma = 2.5$, $D = 1$, and $v_c = 1.75$. (a) Case of white driving noise [$\beta \to 1$ in Eq. (4)] for $\alpha = 0.2$ (solid line) and $\alpha = 0.8$ (dashed line). (b) Case of colored noise ($\beta \neq 1$) for $\beta = \alpha = 0.6$ (internal noise) (solid line) and $\beta = 0.3$ and $\alpha = 0.6$ (external noise) (dashed line). At large values of time $t \to \infty$, all curves tend to zero.

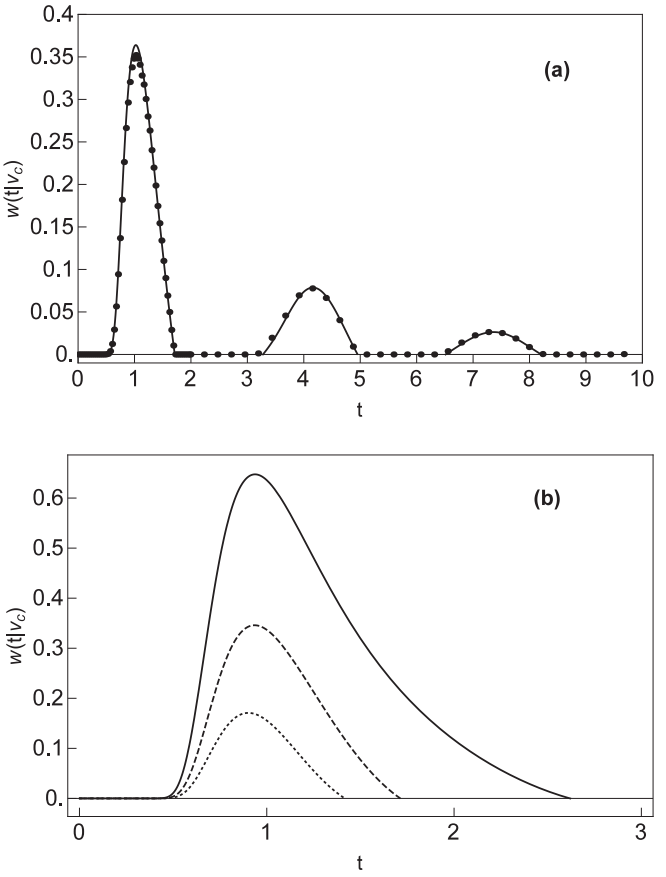

FIG. 4. Behavior of the ISI distribution $w(t|v_c)$ at $\omega = \mu = 1$, $\alpha = 0.2$, and $v_c = 1.75$. (a) Case of internal noise ($\beta = \alpha = 0.2$). The system parameter values are $\gamma = 2.5$ and $k_B T = 0.5$. The solid line is computed from Eqs. (A16)–(A18). The dots represent the calculation data obtained after averaging over 10^2 time steps from the numerical results of a computer simulation of Eq. (A10). The integration time step was set to 0.001 for 10^6 trajectories of $v(t)$. Note that $w(t|v_c) = 0$ at $t_1 \approx 1.7$. (b) Case of an external noise, computed from Eq. (34) at $\beta = 0.6$ and $D = 1$. The parameters are $\gamma = 0.5$ (solid line), $\gamma = 2.5$ (dashed line), and $\gamma = 4$ (dotted line). Note that in those parameter regimes the condition (36) is valid only in a finite-time interval.

preventing diffusion, but forcing oscillations. Thus, the critical memory exponent α_c marks a dynamical transition from the regime where dissipation (normal friction) dominates in the nonlocal friction force to the regime where elastic friction dominates.

Figures 3 and 4 show, for various regimes of system parameters, the typical forms of the ISI distribution $w(t|v_c)$ [see Eq. (34)]. In Fig. 3(a), the case of external white noise [$\beta \to 1$ in Eq. (4)] is considered at various values of the memory exponent α. It can be seen that, contrary to the case of a relatively strong memory ($\alpha = 0.2$), where $w(t|v_c)$ is multimodal, the case of a relatively weak memory ($\alpha = 0.8$) demonstrates a unimodal dependence of $w(t|v_c)$ on time t (at least if the damping coefficient γ is large enough). This circumstance is in accordance with the fact that, as a rule, the damping of the oscillations of $w(t|v_c)$ versus t increases as the memory exponent α grows. Here we recall that in the case of external white noise, condition (30) is fulfilled in the time interval $(0, \infty)$ for all values of other system parameters (including α). Figure 3(b) illustrates, in the shaded domain of the phase diagram (see Fig. 2), the influence of the noise color exponent $\beta \neq 1$ on the behavior of the ISI distribution. For increasing β, the main effect, which can also be observed in Fig. 3(b), consists in a more rapid decrease of $w(t|v_c)$ as a function of t. From Eqs. (B6)–(B15), (34), and (C1) it is easily seen that for large t the probability density $w(t|v_c)$ decays as a power law

$$w(t|v_c) \sim \frac{1}{t^{1+\alpha+\beta}}, \quad \beta \neq 1, \tag{39}$$

demonstrating that such a tendency, i.e., a more rapid decrease of $w(t|v_c)$ in time by increasing β, also occurs in the asymptotic regime $t \to \infty$.

In the unshaded domain of the phase diagram (see Fig. 2), the behavior of the ISI distribution is qualitatively different from the one described above. Namely, in this region of system parameter values the multimodal structure of $w(t|v_c)$ versus time is characterized by time instants where spike firing is not possible [see also Fig. 4(a)]. In this case formula (34)

is applicable only for a finite time interval $(0,t_1)$, where the inequality (30) is valid, i.e., before the first zero of $w(t|v_c)$ in Fig. 4(a). It should be noted that we have been unable to derive an exact ISI distribution for the times $t > t_1$. Therefore, in Appendix A we present an extended model in the complex form (A10). In Fig. 4(a) the dependence of $w(t|v_c)$ on time t computed from Eqs. (A16)–(A18) at $\beta = \alpha = 0.2$ and $\gamma/\omega^{2-\alpha} = 2.5$ is compared with the computer simulation of Eq. (A10) using the program *Mathematica 10* to generate the trajectories of white Gaussian noise. The integration time step Δt was set to 0.001 and 10^6 sample trajectories were used for the evaluation of $w(t|v_c)$. The results of the simulation show good qualitative agreement with the exact values of $w(t|v_c)$ predicted by the extended model (A10). For the case of an external noise the dependence of the ISI distribution $w(t|v_c)$ on time t in the interval $(0,t_1)$ is illustrated in Fig. 4(b) at various values of the damping coefficient γ. It can be seen that by increasing γ in this parameter regime, the peak of $w(t|v_c)$ decreases and the time interval $(0,t_1)$ becomes narrower. More precisely, at $\alpha < \alpha_c$ it follows from Eqs. (34) and (B6) that at increasing γ the time t_1 decreases from π/ω (at $\gamma \to 0$) to zero according to a power law

$$t_1 \simeq \frac{\pi}{\gamma^{1/(2-\alpha)} \sin\left(\frac{\pi}{2-\alpha}\right)}, \quad \gamma \to \infty. \tag{40}$$

Notably in the unshaded domain of the phase diagram (see Fig. 2) the time interval $(0,t_1)$ depends only on the memory kernel and is independent of any external random force $\xi(t)$ [cf. also Figs. 3(a) and 4(b)]. The fact that at the instant t_1 the probability density $w(t|v_c)$ tends to zero is in sharp contrast with the results for the shaded domain of Fig. 2, where $w(t|v_c)$ is always positive for all finite values of time. In a sense, the behavior of the ISI density in the unshaded domain is more similar to the multimodal behavior of $w(t|v_c)$ for the model with an external white noise, where zeros of $w(t|v_c)$ appear at finite-time instants.

Relying on Fig. 2, one can establish the emergence of memory-induced transitions in the shape of the ISI distribution due to variation of the memory exponent. For example, in the case of $\min[\omega^{2-\alpha}\kappa(\alpha)] < \gamma < 2\omega, \omega \leqslant 1$, these transitions are characterized by the following scenario: For small values of the memory exponent $\alpha < \alpha_1$, where α_1 is the first (smallest) solution of the equation $\omega^{2-\alpha}\kappa(\alpha) = \gamma$, the ISI density $w(t|v_c)$ exhibits zeros between peaks. At $\alpha = \alpha_1$ the zeros of $w(t|v_c)$ disappear and in the interval $\alpha_1 < \alpha < \alpha_2$, where α_2 is the second solution of the equation $\omega^{2-\alpha}\kappa(\alpha) = \gamma$, the multimodal behavior of $w(t|v_c)$ is described by Eq. (34). By a further increase of α, at $\alpha = \alpha_2$, a reentrant transition to the ISI distribution occurs, characterized by time instants at which the probability density of spike firing vanishes. In the case of $\gamma > 2\omega$, memory-induced transitions different from those considered above can be observed on the phase diagram in Fig. 2. Namely, in Fig. 2 the dashed line represents, in the case of internal noise at the parameter regime $\omega = \mu = 1$, $k_B T = 0.15$, and $v_c = 1.75$, a critical curve (see also Appendix B)

$$\gamma_{c1}(\alpha) = \omega^{2-\alpha}\kappa_1(\alpha,\rho), \quad \rho = \frac{(v_c - \mu/\omega^2)^2\omega^2}{2k_B T} \tag{41}$$

on which a transition from a bimodal shape of $w(t|v_c)$ to a unimodal shape appears. Thus, by increasing α the ISI distribution undergoes two transitions: from the shape with zeros between peaks to a multimodal one without zeros and further to the unimodal shape. It should be noted that for external noise, the critical curve $\tilde{\gamma}_{c1}(\alpha)$, which determines the transitions between bimodal and unimodal shapes of $w(t|v_c)$, satisfies the relation

$$\tilde{\gamma}_{c1}(\alpha) = \omega^{2-\alpha}\tilde{\kappa}_1(\alpha,\beta,\tilde{\rho}), \quad \tilde{\rho} = \frac{(v_c\omega^2 - \mu)^2}{2D\omega^\beta}, \tag{42}$$

which is different from Eq. (41). An important difference between the critical curves $\gamma_c(\alpha)$ and $\tilde{\gamma}_{c1}(\alpha)$ described by Eqs. (38) and (42), respectively, is that for γ_c the scaling function $\kappa(\alpha)$ depends only on the memory exponent α and as such is quite universal (applicable for both internal and external noises), but for $\tilde{\gamma}_{c1}$, in the scaling function $\tilde{\kappa}(\alpha,\beta,\tilde{\rho})$ an additional dependence on the noise exponent β as well as on the other system parameters occurs. Remarkably, according to Eq. (42), by the time scaling $\omega = 1$ the critical curve $\tilde{\gamma}_{c1}(\alpha,\beta)$ depends on other system parameters only through the single parameter $\tilde{\rho}$. This implies that an increase in the threshold potential v_c can leave the transition point on the phase space (γ-α) unchanged if the noise parameter D (or the input force μ) is increased at the same time so that $\tilde{\rho}$ remains unaffected. In Fig. 5 we illustrate, in the case of an external noise of a fixed value $\tilde{\rho}$, the dependence of the function $\tilde{\kappa}_1(\alpha,\beta,\tilde{\rho})$ on the memory exponent α at various values of the noise exponent β.

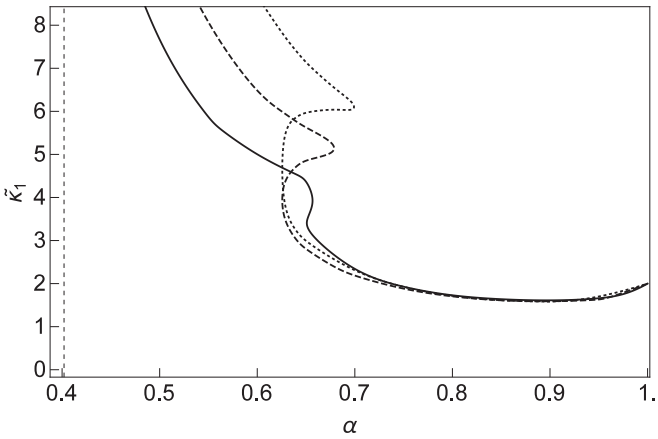

FIG. 5. Dependence of the scaling function $\tilde{\kappa}_1(\alpha,\beta,\tilde{\rho})$ [see also Eq. (42)] on the memory exponent α computed from Eqs. (34), (B6), (B15), and (C3) at different values of the noise exponent β in the case of external noise. The time scaling is determined with $\omega = 1$ and the chosen value of the parameter $\tilde{\rho} = 0.281$. The vertical dashed line indicates the critical memory exponent $\alpha_c \approx 0.402$. The solid line shows $\beta = 0.2$, the dashed line $\beta = 0.6$, and the dotted line $\beta = 0.9$.

A peculiarity of Fig. 5 is the hysteresislike behavior of $\tilde{\kappa}_1(\alpha)$ in the interval $\alpha \in (0.6,0.7)$. If the memory exponent α is greater than 0.7, the dependence of $\tilde{\kappa}_1(\alpha,\beta,\tilde{\rho})$ on β is almost unnoticeable, but for $\alpha < 0.6$ the influence of the noise exponent β is significant. In the last case, a monotonic increase in the function $\tilde{\kappa}_1(\alpha,\beta,\tilde{\rho})$ with an increasing β can be seen. In the region of hysteresis, we observe an interesting behavior of $w(t|v_c)$: As the friction coefficient γ increases, not only one transition from a bimodal to unimodal structure of $w(t|v_c)$ occurs, but we observe three transitions: from a bimodal to a unimodal one, then back to bimodal, and finally a reentrant

transition to a unimodal structure [cf. also Eq. (42)]. Note that the hysteresislike behavior of $\tilde{\kappa}_1(\alpha)$ vs α is quite robust; it exists for a large range of values of $\tilde{\rho}$ and even in the case of an internal noise (see also Fig. 2).

B. Memory-induced resonancelike suppression

We now turn to describing the behavior of the survival probability $F(t)$ [see also Eq. (32)] in the long-time limit $t \to \infty$. Here we recall that $1 - F(\infty)$ gives the probability that a spike is generated in the time interval $(0,\infty)$. In the following, we confine ourselves to the cases where the condition (30) is satisfied in the infinite time interval $t \in (0,\infty)$. From Eqs. (32) and (C2) it follows that in the case of internal noise the survival probability $F(\infty)$ is independent of the memory exponent α:

$$F(\infty) = \mathrm{erf}\left(\frac{v_c\omega^2 - \mu}{\omega\sqrt{2k_BT}}\right). \tag{43}$$

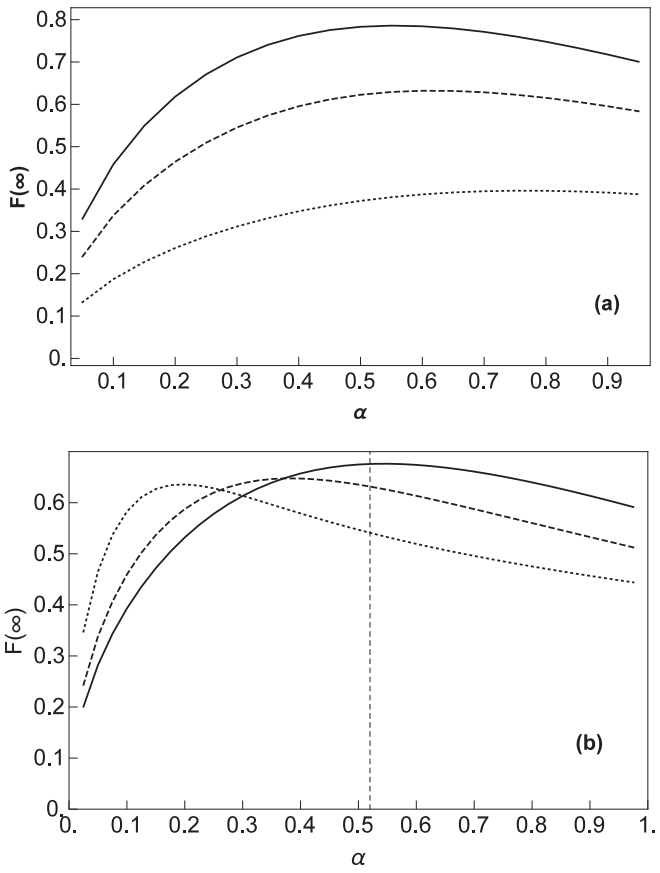

FIG. 6. Dependence of the survival probability $F(\infty)$, computed from Eqs. (32) and (C1), on the memory exponent α. All quantities are dimensionless with time and voltage scaling determined by $\omega = 1$ and $\mu = 1$, respectively. The system parameter values are $D = 1$ and $v_c = 1.5$. (a) Case of white external noise for $\beta = 1$ and $\gamma = 6$ (solid line), $\gamma = 2.5$ (dashed line), and $\gamma = 1$ (dotted). (b) Behavior of $F(\infty)$ for various values of the noise exponent β at $\gamma = 3$: $\beta = 0.9$ (solid line), $\beta = 0.6$ (dashed line), and $\beta = 0.3$ (dotted line). The thin vertical dashed line indicates the value of the memory exponent $\alpha \approx 0.52$, below which the condition (30) is not fulfilled for any $t \in (0,\infty)$. At $\alpha = 0$ all curves tend to zero very fast.

Thus $F(\infty)$ increases monotonically as the temperature T of the heat bath decreases or as the threshold potential v_c increases, which can also be expected from a physical point of view. The case of external noise is more interesting. In Figs. 6(a) and 6(b) the graphs depict, by the time and voltage scaling $\omega = \mu = 1$, the dependence of $F(\infty)$ on the memory exponent α for various values of the noise exponent β and the damping coefficient γ. These graphs show a typical resonancelike behavior of $F(\infty)$ versus α. The phenomenon is more pronounced at higher values of the friction constant $\gamma > 1$ [see also Fig. 6(a)]. As a rule, the maximal value of $F(\infty)$ increases as the value of the damping coefficient γ increases. Thus, at intermediate values of the memory exponent α, the survival probability is significantly enhanced, compared to the cases of weak and strong memory (at least if $\beta = 1$ and $\gamma > 1$). From Fig. 6(b) it can be seen that the memory-induced enhancement of $F(\infty)$ is stronger at smaller values of the noise exponent β, while the positions of the maxima are monotonically shifted to lower α as β decreases. However, it should be noted that in the parameter regime displayed in Fig. 6(b) the resonancelike maxima of $F(\infty)$ are quite formal, since in those regimes the condition (30) at $\alpha < 0.52$ is not fulfilled on the whole semiaxis $t \in (0,\infty)$ and that renders the formula (32) for $\alpha < 0.52$ physically meaningless (if $t \to \infty$). Bearing in mind the results obtained and Eq. (35), one can conclude that in the case of external noise, for sufficiently large values of the damping coefficient γ, the ISI probability density $w(t|v_c)$ is significantly suppressed at moderate values of the memory exponent α in the sense that the probability of spike generation in the time interval $(0,\infty)$, $1 - F(\infty)$, is suppressed at moderate values of α [see also Eq. (35)]. This statement is illustrated in Fig. 7, where in the case of white external noise, three graphs for $w(t|v_c)$ versus time t at different values of α are presented. Finally, we call attention to the fact that while memory shows up as the fundamental

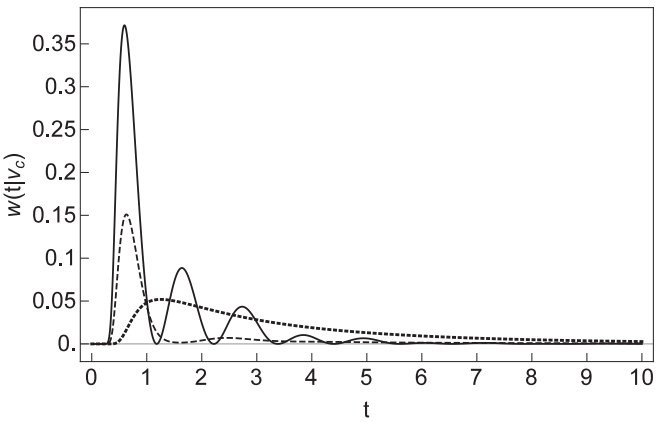

FIG. 7. Memory-induced suppression of the ISI distribution $w(t|v_c)$. The graphs of $w(t|v_c)$ versus time t are computed from Eqs. (34), (B6), (C1), and (C3). All quantities are dimensionless with the time and voltage scaling determined by $\omega = 1$ and $\mu = 1$, respectively. The system parameter values are $D = 1$, $\beta = 1$, $\gamma = 6$, $v_c = 1.5$, and $\alpha = 0.2$ (solid line), $\alpha = 0.5$ (dashed line), and $\alpha = 0.9$ (dotted line). Note the suppression of $w(t|v_c)$ at $\alpha = 0.5$ (dashed line), i.e., the area under the dashed line is smaller than those under other lines.

ingredient leading to a qualitative change in the structure of the ISI distribution, the exponent of the fractional Gaussian noise is not able to change the qualitative aspects of the graphs (an exception is the transition from $\beta \neq 1$ to the white noise limit $\beta \to 1$), but it is important for the quantitative description of the ISIs.

V. CONCLUSION

Motivated by studies of the dynamics of resonant neurons, we have considered a first-passage-time problem for an RF neuron model, where the neuron membrane potential $v(t)$ dynamics is described by a time-nonhomogeneous 1D Langevin equation driven by white Gaussian noise. The dynamical equation of this model is a reduction of a GLE with a power-law memory kernel, where fluctuations of the input, arising from other neurons forming a network with a fractal structure, are expressed as a fractional Gaussian noise. More precisely, the proposed RF model is constructed so that its one-time statistical properties in v space are the same as for the basic GLE. Despite the long history and importance for a large variety of problems in natural sciences, explicit expressions for the FPT density are only known for a few cases [42]. The main aim of the present paper was, using the FPT approach, to obtain the exact formulas for the ISI distribution generated by the model considered. In the noise-induced firing regime, we have been able to derive, for certain system parameter domains, exact analytical expressions of the output ISI density and the probability for the occurrence of an inactive phase (i.e., the probability that the generation of spikes is absent in the whole time domain). As one of our main results, we have established memory-induced transitions in the ISI distribution. For example, in the case of the external white noise, if the damping coefficient is large enough, a decrease of the memory exponent α reproduces transitions between three qualitatively different structures of the ISI distribution (caused by the subthreshold dynamics of the model): from monomodal through bimodal to multimodal densities with several decaying maxima, separated by points where a spike generation is absent. Moreover, we have found a critical memory exponent $\alpha_c \approx 0.402$, below which the ISI density is at all values of other system parameters multimodal with decaying maxima. It should be noted that in the multimodal regimes, the first maximum is mostly very sharp and corresponds to the ISIs within a burst of spike generation. Thus, this regime assumes a bursting effect, actually observed in natural resonant neurons [60]. We have shown that there is no pronounced qualitative difference between the memory-induced transitions for the shape of the ISI density generated by internal and external noises. An exception is white external noise, at which the formula obtained for the ISI distribution [see Eq. (34)] is applicable in the time interval $(0,\infty)$ for the whole system parameters space. Furthermore, another interesting result is that for external noises, the model predicts, at intermediate values of the memory exponent α, a suppression of the spike generation. Such behavior of the ISI distribution contrasts with that of the model with internal noise, where such a memory-induced suppression is absent. This effect deserves deeper investigations in the neurobiological context in the future. One should take care not to confuse the phenomenon of inverse stochastic resonance considered in the context of a single Hodgkin-Huxley neuron [61] with the memory-induced resonancelike suppression of spike generation considered in this paper. The former reveals that a neuron's firing rate may undergo a pronounced minimum as the noise intensity increases, but in our model such a resonancelike dependence on the noise intensity is absent.

Although the theoretical results of the present paper are restricted with the conditions for the reset state [see Eq. (7)], the model considered here can nevertheless also be of interest from the experimental point of view, since the control parameter is the input force μ, which can be easily adjusted in possible experiments. However, a further detailed study, especially a comparison of the FPT densities predicted by both models [Eq. (1) and Eqs. (8) and (9)], is necessary. Undoubtedly, the ultimate verification of the relevance of the proposed model for neuroscience lies with experimentalists.

We believe that our exact results can be a good starting point for investigations of more elaborate model systems for neuronal dynamics in networks and can also be of interest in other fields where issues of excitability, memory, and colored noise play an important role, e.g., in biophysics and physical chemistry [62].

ACKNOWLEDGMENTS

This work was supported by the International Atomic Energy Agency CPR F13016 Grant No. RC-20428 and by the European Union through the European Regional Development Fund. The authors would like to thank the anonymous reviewers for their valuable comments.

APPENDIX A: THE SDE (8) IN v SPACE

1. Functions $A(t)$ and $D(t)$ for the model (8)

In order to find the functions $A(t)$ and $D(t)$ for Eq. (8) we first derive a Fokker-Planck-type master equation in v space for the position conditional probability density $p(v,t|v_0,\dot{v}_0,0)$ associated with the GLE (1). Using the characteristic function method, such a master equation has previously been found in [13]. Here we will use an alternative method presented in [46,63].

For a given realization of the noise $\phi(t)$,

$$\phi(t) \equiv \int_0^t \dot{H}(t-\tau)\xi(\tau)d\tau, \tag{A1}$$

Eq. (13) describes a flow in v space. The indicator function of this flow

$$f(v,t) = \delta(v(t) - v), \tag{A2}$$

where $v(t)$ is the solution to Eq. (13), evolves in time according to the stochastic Liouville equation

$$\frac{\partial}{\partial t} f(v[\phi],t) = -\frac{\partial}{\partial v}\left[f(v[\phi],t)\frac{\partial v[\phi]}{\partial t}\right], \tag{A3}$$

where $v[\phi]$ marks that $v(t)$ is a functional of the noise $\phi(t)$. The probability density of the fixed realization v at time t, $p(v,t|v_0,\dot{v}_0,0)$, can be obtained by averaging the indicator function over the distribution of the colored noise $\phi(t)$ [46,63],

namely,

$$p(v,t|v_0,\dot{v}_0,0) = \langle f(v[\phi],t)\rangle_\phi. \tag{A4}$$

Here the subscript ϕ is a reminder that the probability density of the colored noise $\phi(t)$ has to be employed in the calculation of the average. Now, by substituting Eq. (13) into Eq. (A3), the equation satisfied by $p(v,t|v_0,\dot{v}_0,0)$ reads

$$\frac{\partial}{\partial t}p(v,t|v_0,\dot{v}_0,0) = -\langle\dot{v}(t)\rangle\frac{\partial}{\partial v}p(v,t|v_0,\dot{v}_0,0) - \frac{\partial}{\partial v}\langle f(v[\phi],t)\phi(t)\rangle_\phi. \tag{A5}$$

Since $\phi(t)$ is a zero-mean Gaussian noise, the correlator $\langle f(v[\phi],t)\phi(t)\rangle_\phi$ is given by the Furutsu-Novikov formula [63–65]

$$\begin{aligned}\langle f(v[\phi],t)\phi(t)\rangle_\phi &= -\int_0^t \langle\phi(t)\phi(\tau)\rangle \times\left\langle\frac{\partial f(v[\phi],t)}{\partial v[\phi]}\frac{\delta v[\phi]}{\delta\phi(\tau)}\right\rangle d\tau \\ &= -\int_0^t \langle\phi(t)\phi(\tau)\rangle d\tau\frac{\partial}{\partial v}p(v,t|v_0,\dot{v}_0,0),\end{aligned} \tag{A6}$$

where the functional derivative $\delta v[\phi]/\delta\phi(\tau) = 1$ can be obtained from Eqs. (12) and (A1). Next, substituting Eq. (A6) into Eq. (A5) and using Eqs. (A1), (20), and (21), we finally find that $p(v,t|v_0\dot{v}_0,0)$ satisfies the Fokker-Planck-type master equation

$$\frac{\partial}{\partial t}p(v,t|v_0,\dot{v}_0,0) = -\langle\dot{v}(t)\rangle\frac{\partial}{\partial v}p(v,t|v_0,\dot{v}_0,0) + \frac{1}{2}\dot{\sigma}_{vv}(t)\frac{\partial^2}{\partial v^2}p(v,t|v_0,\dot{v}_0,0). \tag{A7}$$

Notably, this equation is just the same as the master equation obtained in [13]. Since Eq. (A7) is a well-defined master equation, by inspection, in the case of $\dot{\sigma}_{vv}(t) \geqslant 0$ it can be reinterpreted as resulting from the SDE

$$dv(t) = \langle\dot{v}(t)\rangle dt + \sqrt{\dot{\sigma}_{vv}(t)}\,dW(t), \tag{A8}$$

where $W(t)$ is a Wiener process. Thus, comparing this equation with Eq. (8), we can identify the functions $A(t)$ and $D(t)$ with $\langle\dot{v}(t)\rangle$ and $\frac{1}{2}\dot{\sigma}_{vv}(t)$, respectively. It should be pointed out that a similar reduction of a GLE to a one-dimensional SDE was previously considered in Ref. [63], where possible applications were also discussed.

Finally, we note that the SDE (8) with Eq. (9) can be obtained in a more direct way. Due to the Gaussian property of the noise $\xi(t)$ and the linearity of Eq. (1), the conditional probability density $p(v,t|v_0,\dot{v}_0,0)$ for an unrestricted process $v(t)$ must also be Gaussian [46], i.e.,

$$p(v,t|v_0,\dot{v}_0,0) = \frac{1}{\sqrt{2\sigma_{vv}(t)}}\exp\left[-\frac{[v-\langle v(t)\rangle]^2}{2\sigma_{vv}(t)}\right], \tag{A9}$$

with Eqs. (14) and (18). From Eq. (A9) it follows immediately that the dynamical equation for $p(v,t|v_0,\dot{v}_0,0)$ is exactly the same as Eq. (A7). Interpreting this dynamical equation as a time-dependent FPE, we obtain the equivalent SDE (8) with Eq. (9).

2. Extended model

In Sec. IV A we have shown that in some parameter regimes the cross correlation $\sigma_{yv}(t) = \frac{1}{2}\dot{\sigma}_{vv}(t)$ becomes negative valued in a set of discrete time intervals (t_{2n-1},t_{2n}), where $n = 1,2,\ldots,N$. To access the voltage $v(t)$ evolution in the whole time semiaxis $t \in (0,\infty)$, we postulated that $v(t)$ dynamics can be described by an extended model in the complex form

$$\frac{d}{dt}z(t) = \langle\dot{v}(t)\rangle + \sqrt{\dot{\sigma}_{vv}(t)}dW(t), \tag{A10}$$

where

$$z(t) = v(t) + ib(t). \tag{A11}$$

Here $z(t)$ is a complex-valued variable that describes the activity of the neuron. The real part $v(t) = \mathrm{Re}\ z(t)$ is the membrane voltage. The imaginary part $b(t) = \mathrm{Im}\ z(t)$ is a currentlike auxiliary variable. The model is completed upon specification of the fire-and-reset rule, which reads as follows: If $\mathrm{Re}\ z(t) = v_c$, then a spike is considered to have occurred at time t and $z(t)$ is reset to the state [cf. Eq. (7)]

$$z = v_r = \frac{\mu}{\omega^2}, \quad \dot{z} = \dot{v}_r = 0. \tag{A12}$$

To solve the FPT problem from the reset state (A12) to $\mathrm{Re}\ z = v_c > \frac{\mu}{\omega^2}$ we use, in the case of $\dot{\sigma}_{vv}(t) \geqslant 0$, that the stochastic process $\mathrm{Re}\ z(t) = v(t)$ is described by the FPE (A7). As by the initial conditions (A12) the average $\langle\dot{v}(t)\rangle$ vanishes [see also Eq. (15)], $\langle\dot{v}(t)\rangle = 0$, we obtain from Eqs. (A10) and (A11) that the conditional probability density $p(v,t|v_0,\dot{v}_0,0)$ for the process with an absorbing boundary at $v = v_c$ can be found as

$$p(v,t|v_0,\dot{v}_0,0) = p(v,t_{2n-1}|v_0,\dot{v}_0,0) \tag{A13}$$

if $t \in (t_{2n-1},t_{2n})$ and in the intervals $t \in (t_{2n},t_{2n+1})$ it is given by the solution of Eq. (A7) with the initial condition

$$p(v,t_{2n}|v_0,\dot{v}_0,0) = p(v,t_{2n-1}|v_0,\dot{v}_0,0) \tag{A14}$$

in the presence of an absorbing boundary at $v = v_c$,

$$p(v_c,t|v_0,\dot{v}_0,0) = 0. \tag{A15}$$

Now the survival probability $F(t)$ can be found analogously to the case considered in Sec. III B. Finally, we obtain

$$F(t) = \mathrm{erf}\left\{\left(v_c - \frac{\mu}{\omega^2}\right)\left[2\left(\sigma_{vv}(t) + \sum_{k=1}^{2n}(-1)^{k+1}\sigma_{vv}(t_k)\right)\right]^{-1/2}\right\} \tag{A16}$$

if $t_{2n+1} \geqslant t \geqslant t_{2n}$ and

$$F(t) = \mathrm{erf}\left\{\left(v_c - \frac{\mu}{\omega^2}\right) \times\left[2\sum_{k=1}^{2n-1}(-1)^{k+1}\sigma_{vv}(t_k)\right)\right]^{-1/2}\right\} \tag{A17}$$

if $t_{2n} \geqslant t \geqslant t_{2n-1}$, $n = 1,2,\ldots$. The corresponding ISI distribution $w(t|v_c)$ is given by

$$w(t|v_c) = -\dot{F}(t). \tag{A18}$$

Note that in the case $t \leqslant t_1$ the survival probability $F(t)$ is determined by Eq. (32).

APPENDIX B: DERIVATION OF EQS. (12)–(15) AND FORMULAS FOR THE RELAXATION FUNCTIONS

1. Formal solution of the GLE (1)

The GLE (1) can be formally solved by means of Laplace transformation. Taking into account the deterministic initial conditions $v_0 = v(0)$ and $\dot{v}_0 = \dot{v}(0)$, the evolution of the Laplace transform $\hat{v}(s)$ of the voltage $v(t)$ reads

$$\hat{v}(s) = \frac{1}{s}(\mu - \omega^2 v_0)\hat{H}(s) + \dot{v}_0\hat{H}(s) + \hat{\xi}(s)\hat{H}(s) + \frac{v_0}{s}, \tag{B1}$$

where

$$\hat{H}(s) := \frac{1}{s^2 + \gamma s^\alpha + \omega^2}, \tag{B2}$$

$\hat{\xi}(s)$ is the Laplace transform of the noise $\xi(t)$, and we have used the fact that the Laplace transform of the fractional derivative $d^\alpha v(t)/dt^\alpha$ is given by

$$\widehat{\left(\frac{d^\alpha}{dt^\alpha}v\right)} = s^\alpha \hat{v}(s) - v_0 s^{\alpha-1}. \tag{B3}$$

From Eqs. (B1) and (B2), an expression for the voltage $v(t)$ can be found by means of the inverse Laplace transformation

$$v(t) = v_0 + \dot{v}_0 H(t) + (\mu - \omega^2 v_0)\int_0^t H(\tau)d\tau + \int_0^t H(t-\tau)\xi(\tau)d\tau, \tag{B4}$$

where the response function $H(t)$ is the Laplace inversion of $\hat{H}(s)$. Again, from Eq. (B4) one gets Eqs. (12) and (14). Using that

$$H(0) = \lim_{s\to\infty}[s\hat{H}(s)] = 0, \tag{B5}$$

the formulas (13) and (15) can be obtained from Eq. (B4) by differentiation.

2. Formulas for the relaxation functions

The relaxation functions $H(t)$, $G(t)$, and $M(t)$ in Eqs. (18)–(24) can be obtained by means of the Laplace transformation technique. To evaluate the inverse Laplace transform of $\hat{H}(s)$ [see Eq. (B2)], we use the residue theorem method described in [66]. The inverse Laplace transform gives

$$H(t) = \frac{2}{\sqrt{u^2+v^2}}\mathrm{Im}[e^{i\theta}e^{-(v-i\omega^*)t}] + \frac{\gamma\,\sin(\alpha\pi)}{\pi}\int_0^\infty \frac{r^\alpha e^{-rt}dr}{B(r)}. \tag{B6}$$

Here $s_{1,2} = -v \pm i\omega^*$ ($v > 0$ and $\omega^* > 0$) are the pair of complex-conjugate zeros of the equation

$$s^2 + \gamma s^\alpha + \omega^2 = 0, \tag{B7}$$

where Eq. (B7) is defined by the principal branch of s^α. The quantities u, v, θ, and $B(r)$ are determined by

$$u = -2v + \frac{\gamma\alpha\,\cos[(1-\alpha)\varphi]}{(v^2+\omega^{*2})^{(1-\alpha)/2}}, \tag{B8}$$

$$v = 2\omega^* - \frac{\gamma\alpha\,\sin[(1-\alpha)\varphi]}{(v^2+\omega^{*2})^{(1-\alpha)/2}}, \tag{B9}$$

with

$$\varphi = \pi + \arctan\left(-\frac{\omega^*}{v}\right), \tag{B10}$$

$$\theta = \arctan\left(\frac{u}{v}\right), \tag{B11}$$

and

$$B(r) = [r^2 + \gamma r^\alpha\cos(\alpha\pi) + \omega^2]^2 + \gamma^2 r^{2\alpha}\sin^2(\alpha\pi). \tag{B12}$$

The relaxation function $H(t)$ can be represented via Mittag-Leffler-type special functions [56]. However, as in the last case the numerical calculations are very complicated, so we suggest, apart from possible representations via Mittag-Leffler functions, a numerical treatment of Eq. (B6). It should be noted that the representation (B6) of the relaxation function $H(t)$ was previously used in an analysis of the energetic stability of a fractional oscillator with multiplicative noise [67].

From Eqs. (25) and (B6) one can conclude that the relaxation function $G(t)$ [see Eq. (25)] is given by

$$G(t) = \frac{2}{\sqrt{u^2+v^2}}\mathrm{Im}\left[\frac{e^{i\theta}e^{-(v-i\omega^*)t}}{(v-i\omega^*)}\right] + \frac{\gamma\,\sin(\alpha\pi)}{\pi}\int_0^\infty \frac{e^{-rt}dr}{r^{1-\alpha}B(r)}. \tag{B13}$$

To derive a convenient representation of $M(t)$ defined by Eq. (21), we start from a Laplace transform $\hat{M}(s)$ of the function $M(t)$ [see also Eqs. (B2) and (4)],

$$\hat{M}(s) = \frac{Ds^{\beta-1}}{s^2 + \gamma s^\alpha + \omega^2}. \tag{B14}$$

Using the residue theorem method, the inverse Laplace transform gives

$$M(t) = D\left\{\frac{2}{\sqrt{u^2+v^2}}\mathrm{Im}[(-v+i\omega^*)^{\beta-1}e^{i\theta}e^{-(v-i\omega^*)t}] + \frac{1}{\pi}\int_0^\infty \frac{r^{\beta-1}e^{-rt}}{B(r)}\{(r^2+\omega^2)\,\sin(\beta\pi) + \gamma r^\alpha\,\sin[(\beta-\alpha)\pi]\}dr\right\}. \tag{B15}$$

From Eq. (B15) it follows that in the case of external white noise (i.e., $\beta = 1$) $M(t) = DH(t)$, which can be expected. So in this particular case the condition (30) is fulfilled in the time interval $(0,\infty)$ for all values of other system parameters.

3. Critical curves (38) and (41)

Using that the relaxation function $H(t)$ is the solution of the equation

$$\ddot{H}(t) + \gamma \frac{d^\alpha}{dt^\alpha} H(t) + \omega^2 H(t) = 0 \tag{B16}$$

with initial conditions

$$H(0) = 0, \quad \dot{H}(0) = 1, \tag{B17}$$

we obtain by the time scaling $\tilde{t} = t\omega$ that $H(t)$ and γ satisfy the scaling laws

$$\gamma = \omega^{2-\alpha}\tilde{\gamma},$$
$$H(t;\gamma,\alpha,\omega) = \frac{1}{\omega} H(\tilde{t};\tilde{\gamma},\alpha,1). \tag{B18}$$

Thus the conditions (37) for the critical curve $\tilde{\gamma}_c(\alpha)$ [Eq. (38)] can be represented in the form

$$H(\tilde{t}_1;\tilde{\gamma}_c,\alpha,1) = 0, \quad \frac{\partial}{\partial \tilde{t}} H(\tilde{t};\tilde{\gamma}_c,\alpha,1)_{|\tilde{t}=\tilde{t}_1} = 0, \tag{B19}$$

where the time instant $t_1 = \tilde{t}_1/\omega > 0$ corresponds to the first zero of $H(t)$ on the critical curve. From Eq. (B19) it follows that both the critical curve $\tilde{\gamma}_c(\alpha)$ and $\tilde{t}_1(\alpha)$ only depend on the memory exponent α. Thus Eq. (38) is recovered.

To obtain Eq. (41) we use similar arguments as above. The critical curve $\gamma_{c1}(\alpha)$ [Eq. (41)] is determined by the equations

$$\dot{w}(t|v_c) = 0, \quad \ddot{w}(t|v_c) = 0. \tag{B20}$$

Defining

$$\rho = \frac{\omega^2\left(v_c - \frac{\mu}{\omega^2}\right)^2}{2k_B T} \tag{B21}$$

and

$$f(t) \equiv f(t;\gamma,\alpha,\omega) = \frac{\omega^2}{k_B T}\sigma_{vv}(t), \tag{B22}$$

from Eq. (34) we obtain

$$w(t;\gamma,\rho,\alpha,\omega) \equiv w(t|v_c) = \frac{\sqrt{\rho}\,\dot{f}(t)}{\sqrt{\pi}\,f(t)^{3/2}} \exp\left[-\frac{\rho}{f(t)}\right]. \tag{B23}$$

From Eqs. (22), (25), and (B18) one can see that

$$f(t;\gamma,\alpha,\omega) = f(\tilde{t};\tilde{\gamma},\alpha,1) \tag{B24}$$

and consequently

$$w(t;\gamma,\rho,\alpha,\omega) = \omega w(\tilde{t};\tilde{\gamma},\rho,\alpha,1). \tag{B25}$$

Using Eq. (B25), the conditions (B20) for the critical curve $\gamma_{c1}(\alpha)$ [Eq. (41)] can be written as

$$\frac{\partial}{\partial \tilde{t}} w(\tilde{t};\tilde{\gamma}_{cr},\rho,\alpha,1)_{|\tilde{t}=\tilde{t}_1} = 0,$$
$$\frac{\partial^2}{\partial \tilde{t}^2} w(\tilde{t};\tilde{\gamma}_{cr},\rho,\alpha,1)_{|\tilde{t}=\tilde{t}_1} = 0. \tag{B26}$$

Thus, from (B26) and (B18) it follows that

$$\gamma_{c1} = \omega^{2-\alpha}\tilde{\gamma}_{cr}(\alpha,\rho), \tag{B27}$$

which is equivalent to Eq. (41). Finally, we note that Eq. (42) for the critical curve $\tilde{\gamma}_{c1}(\alpha)$ can be found, starting from Eq. (34), analogously to the derivation of $\gamma_{c1}(\alpha)$.

APPENDIX C: FORMULAS FOR THE VARIANCE

Here the exact expression for the computation of the variance $\sigma_{vv}(t)$ [see Eq. (18)], which determines the behavior of the ISI density (34) and the survival probability (32), is presented. From Eqs. (18) and (B6) it follows that in the long-time limit $t \to \infty$ the variance σ_{vv} is given by

$$\sigma_{vv}(\infty) = \frac{4}{\sqrt{u^2+v^2}} \mathrm{Im}[e^{i\theta}\hat{M}(v - i\omega^*)] + \frac{2\gamma\,\sin(\pi\alpha)}{\pi}\int_0^\infty \frac{r^\alpha \hat{M}(r)}{B(r)} dr, \tag{C1}$$

where $\hat{M}(s)$ is determined by Eq. (B14). In the case of internal noise $\beta = \alpha$, the formula (C1) reduces to the equation [see also Eqs. (4)–(6) and (22)]

$$\sigma_{vv}(\infty) = \frac{D}{\gamma\omega^2} = \frac{k_B T}{\omega^2}. \tag{C2}$$

For finite times, from Eqs. (18), (B6), and (B15) we obtain

$$\sigma_{vv}(t) = \sigma_{vv}(\infty) - 2D\left\{\frac{\gamma\,\sin(\alpha\pi)}{\pi^2}\int_0^\infty \frac{r^\alpha e^{-rt}}{B(r)}\int_0^\infty \frac{e^{-r't}r'^{\beta-1}f(r')}{(r+r')B(r')}dr\,dr' + \frac{2}{\pi\sqrt{u^2+v^2}} \times \mathrm{Im}\left[e^{i\theta}\int_0^\infty \frac{e^{-(r+v-i\omega^*)t}}{B(r)(r+v-i\omega^*)}[(-v+i\omega^*)^{\beta-1}\gamma r^\alpha \sin(\alpha\pi) + r^{\beta-1}f(r)]dr\right] + \frac{1}{v(u^2+v^2)}\mathrm{Im}\left[e^{i\theta}(-v+i\omega^*)^{\beta-1}e^{-(2v-i\omega^*)t}\left(\sin(\omega^* t+\theta) + \frac{v\,\sin(\omega^* t+\theta) + \omega^*\cos(\omega^* t+\theta)}{v-i\omega^*}\right)\right]\right\}, \tag{C3}$$

where

$$f(r) = (r^2+\omega^2)\sin(\beta\pi) + \gamma\, r^\alpha \sin[(\beta-\alpha)\pi]. \tag{C4}$$

Finally, we note that although the formula (C3) is valid for both internal and external driving noises, in the case of internal noise it is more convenient to use Eq. (22) with Eqs. (B6) and (B13).

[1] L. Gammaitoni, P. Hänggi, P. Jung, and F. Marchesoni, Rev. Mod. Phys. **70**, 223 (1998).
[2] R. Mankin, K. Laas, T. Laas, and E. Reiter, Phys. Rev. E **78**, 031120 (2008).
[3] P. Reimann, Phys. Rep. **361**, 57 (2002).
[4] R. Mankin, R. Tammelo, and D. Martila, Phys. Rev. E **64**, 051114 (2001).
[5] S. C. Kou and X. S. Xie, Phys. Rev. Lett. **93**, 180603 (2004).
[6] R. Mankin, K. Laas, and N. Lumi, Phys. Rev. E **88**, 042142 (2013).
[7] R. Mankin, K. Laas, N. Lumi, and A. Rekker, Phys. Rev. E **90**, 042127 (2014).
[8] A. Fiasconaro and B. Spagnolo, Phys. Rev. E **80**, 041110 (2009).
[9] R. Mankin, E. Soika, A. Sauga, and A. Ainsaar, Phys. Rev. E **77**, 051113 (2008).
[10] C. C. Bloch, *Classical and Quantum Oscillator* (Wiley, New York, 1997).
[11] S. Burov and E. Barkai, Phys. Rev. E **78**, 031112 (2008).
[12] A. D. Viñales and M. A. Despósito, Phys. Rev. E **73**, 016111 (2006).
[13] K. G. Wang and M. Tokuyama, Physica A **265**, 341 (1999).
[14] W. Götze and M. Sperl, Phys. Rev. Lett. **92**, 105701 (2004).
[15] E. Lutz, Phys. Rev. E **64**, 051106 (2001).
[16] W. Götze and L. Sjögren, Rep. Prog. Phys. **55**, 241 (1992).
[17] T. Carlsson, L. Sjögren, E. Mamontov, and K. Psiuk-Maksymowicz, Phys. Rev. E **75**, 031109 (2007).
[18] S. C. Weber, A. J. Spakowitz, and J. A. Theriot, Phys. Rev. Lett. **104**, 238102 (2010).
[19] Q. Gu, E. A. Schiff, S. Grebner, F. Wang, and R. Schwarz, Phys. Rev. Lett. **76**, 3196 (1996).
[20] I. Goychuk, Phys. Rev. E **80**, 046125 (2009).
[21] I. M. Tolić-Nørrelykke, E.-L. Munteanu, G. Thon, L. Oddershede, and K. Berg-Sørensen, Phys. Rev. Lett. **93**, 078102 (2004).
[22] R. Granek and J. Klafter, Phys. Rev. Lett. **95**, 098106 (2005).
[23] S. V. Muniandy, W. X. Chew, and C. S. Wong, Phys. Plasmas **18**, 013701 (2011).
[24] T. Neusius, I. Daidone, I. M. Sokolov, and J. C. Smith, Phys. Rev. Lett. **100**, 188103 (2008).
[25] Y. Gefen, A. Aharony, and S. Alexander, Phys. Rev. Lett. **50**, 77 (1983).
[26] G. L. Gerstein and B. Mandelbrot, Biophys. J. **4**, 41 (1964).
[27] A. N. Burkitt, Biol. Cybern. **95**, 1 (2006).
[28] A. N. Burkitt, Biol. Cybern. **95**, 97 (2006).
[29] N. Brunel, V. Hakim, and M. J. E. Richardson, Phys. Rev. E **67**, 051916 (2003).
[30] E. Salinas and T. J. Sejnowski, J. Neurosci. **20**, 6193 (2000).
[31] N. Brunel, F. S. Chance, N. Fourcaud, and L. F. Abbott, Phys. Rev. Lett. **86**, 2186 (2001).
[32] J. W. Middleton, M. J. Chacron, B. Lindner, and A. Longtin, Phys. Rev. E **68**, 021920 (2003).
[33] B. Lindner, Phys. Rev. E **69**, 022901 (2004).
[34] M. J. E. Richardson, Biol. Cybern. **99**, 381 (2008).
[35] F. Droste and B. Lindner, Biol. Cybern. **108**, 825 (2014).
[36] T. Schwalger, F. Droste, and B. Lindner, J. Comput. Neurosci. **39**, 29 (2015).
[37] F. Müller-Hansen, F. Droste, and B. Lindner, Phys. Rev. E **91**, 022718 (2015).
[38] T. Schwalger and B. Lindner, Phys. Rev. E **92**, 062703 (2015).
[39] A. L. Hodgkin and A. F. Huxley, J. Physiol. **117**, 500 (1952).
[40] L. A. da Silva and R. D. Vilela, Phys. Rev. E **91**, 062702 (2015).
[41] E. M. Izhikevich, Neural Networks **14**, 883 (2001).
[42] T. Verechtchaguina, I. M. Sokolov, and L. Schimansky-Geier, Phys. Rev. E **73**, 031108 (2006).
[43] I. Erchova, G. Kreck, U. Heinemann, and A. V. M. Herz, J. Physiol. **560**, 89 (2004).
[44] A. M. Lacasta, F. Sagues, and J. M. Sancho, Phys. Rev. E **66**, 045105(R) (2002).
[45] C. F. Stevens and A. M. Zador, Nat. Neurosci. **1**, 210 (1998).
[46] V. J. Klyatskin, *Lectures on Dynamics of Stochastic Systems* (Elsevier, London, 2011).
[47] R. Mankin and N. Lumi, Phys. Rev. E **93**, 052143 (2016).
[48] R. Mankin and A. Rekker, Phys. Rev. E **94**, 062103 (2016).
[49] A. D. Dorval, G. S. Russo, T. Hashimoto, W. Xu, W. M. Grill, and J. L. Vitek, J. Neurophysiol. **100**, 2807 (2008).
[50] R. Sirovich, L. Sacerdote, and A. Villa, Math. Biosci. Eng. **11**, 385 (2014).
[51] D. W. Zhou, D. D. Mowrey, P. Tang, and Y. Xu, Phys. Rev. Lett. **115**, 108103 (2015).
[52] G. Werner, Front. Physiol. **1**, 15 (2010).
[53] N. Kadmon Harpaz, T. Flash, and I. Dinsten, Neuron **81**, 452 (2014).
[54] B. Hutcheon, R. M. Miura, and E. Puil, J. Neurophysiol. **76**, 683 (1996).
[55] C. Pedroarena and R. R. Llinas, Proc. Natl. Acad. Sci. USA **94**, 724 (1997).
[56] I. Podlubny, *Fractional Differential Equations* (Academic, San Diego, 1999).
[57] R. Kubo, Rep. Prog. Phys. **29**, 255 (1966).
[58] S. C. Lim and S. V. Muniandy, Phys. Rev. E **66**, 021114 (2002).
[59] A. Molini, P. Talkner, G. G. Katul, and A. Porporato, Physica A **390**, 1841 (2011).
[60] T. Verechtchaguina, L. Schimansky-Geier, and I. M. Sokolov, Phys. Rev. E **70**, 031916 (2004).
[61] B. S. Gutkin, J. Jost, and H. C. Tuckwell, Naturwissenschaften **96**, 1091 (2009).
[62] B. Lindner, J. Garcia-Ojalvo, A. Neiman, and L. Schimansky-Geier, Phys. Rep. **392**, 321 (2004).
[63] W. Olivares-Rivas and P. J. Colmenares, Physica A **458**, 76 (2016).
[64] K. Furutzu, J. Res. Natl. Inst. Stand. Technol. **67D**, 303 (1963).
[65] E. A. Novikov, Sov. Phys.—JETP **20**, 1290 (1965).
[66] S. Kempfle, J. Schäfler, and H. Beyer, Nonlinear Dyn. **29**, 99 (2002).
[67] R. Mankin and A. Rekker, Phys. Rev. E **81**, 041122 (2010).